IBRACON Structures and Materials Journal
Revista IBRACON de Estruturas e Materiais
ISSN 1983-4195 ismj.org

ORIGINAL ARTICLE

Impact of carbonation on reinforced concrete structures, considering the increase of CO_2 due to climate change in Brazil

Impacto da carbonatação nas estruturas de concreto armado, considerando o aumento de CO_2 causado pelas mudanças climáticas no Brasil

Chiara Pinheiro Teodoro[a]
Rogério Carrazedo[a]

[a]Universidade de São Paulo – USP, Escola de Engenharia de São Carlos, Departamento de Engenharia de Estruturas, São Carlos, SP, Brasil

Received 15 July 2024
Revised 03 October 2024
Accepted 21 October 2024

Abstract: Corrosion in reinforced concrete structures has become a growing concern, primarily due to climate change-related factors such as the rise of carbon dioxide levels, temperature fluctuations, and altered precipitation patterns. To address this, regional assessments are vital due to varying environmental impacts. This study examines corrosion in Brazil, focusing on urban CO_2 levels, employing NBR 6118 (2023) to predict depassivation, initial cracks, and failure due to excessive displacement (Serviceability Limit State). Results indicate a 50% depassivation probability within 13 years for a 2.5 cm concrete cover in the worst-case scenario. Additionally, the diameter of reinforcements greatly influences failure probability for excessive displacement, with a 311% increase over 45 years using a 5 mm diameter instead of 10 mm. These findings underscore the urgency of adapting construction practices to consider accelerated carbonation rates in urban environments and the need for ongoing research to refine predictive models and update construction standards accordingly.

Keywords: carbonation, reinforced concrete, Monte Carlo simulation, Finite Element Method based on Positions, climate change.

Resumo: A corrosão em estruturas de concreto armado tem se tornado uma preocupação crescente, principalmente devido aos fatores relacionados às mudanças climáticas, como o aumento dos níveis de dióxido de carbono, mudanças de temperatura e precipitação. A fim de aplicar essas mudanças a estrutura, avaliações regionais são essenciais devido aos impactos ambientais variados. Este estudo examina a corrosão no Brasil, utilizando os níveis urbanos de CO_2, utilizando a NBR 6118 (2023) para prever a despassivação, as fissuras iniciais e a falha devido a deslocamentos excessivos (Estados Limites de Serviço). Os resultados indicam uma probabilidade de despassivação de 50% em 13 anos para um cobrimento de 2,5 cm no pior cenário. Além disso, a probabilidade de falha por deslocamento excessivo sofre uma influência significativamente do diâmetro das armaduras, com um aumento de 311% ao longo de 45 anos ao usar um diâmetro de 5 mm em vez de 10 mm. Embora preliminar, este estudo também serve como um alerta para as construções futura e existentes, destacando a necessidade de pesquisas contínuas.

Palavras-chave: corrosão, concreto armado, simulação de Monte Carlo, Método dos Elementos Finitos baseado em Posições, mudança climática.

How to cite: C. P. Teodoro and R. Carrazedo, "Impact of carbonation on reinforced concrete structures, considering the increase of CO_2 due to climate change in Brazil," *Rev. IBRACON Estrut. Mater.*, vol. 18, no. 1, e18114, 2025, https://doi.org/10.1590/S1983-41952025000800014.

Corresponding author: Chiara Pinheiro Teodoro. E-mail: chiarapteodoro@usp.br
Financial support: This research was funded by the Brazilian National Council for Scientific and Technological Development (CNPq, grant n. 302885/2022-6) and the Coordination for the Improvement of Higher Education Personnel (CAPES) Finance Code 001 and grant 2023/13093-9, São Paulo Research Foundation (FAPESP).
Conflict of interest: Nothing to declare.
Data Availability: The data that support the findings of this study are available from the corresponding author upon reasonable request.colarItens

1 INTRODUCTION

Reinforced concrete (RC) structures, widely utilized in Brazil, are well-known for their durability and low maintenance requirements; however, they are not impervious to degradation. One of the primary causes of degradation in RC structures is corrosion induced by aggressive agents, e.g. chlorides and carbon dioxide [1], [2].

Corrosion not only affects the safety and comfort of the occupants of the compromised structures but also has economic implications. These consequences are expected to escalate in the future due to the worsening effects of climate change on corrosion processes over time. Hence, proactive preparation for these challenges is of utmost importance.

Environmental conditions play a crucial role in the corrosion of RC structures. Factors such as temperature, humidity, the concentration of carbon dioxide (CO_2) and chlorides (Cl^-), the duration of rain or snow periods, as well as other factors such as water-to-cement ratio (W/C), concrete compressive strength and cover depth significantly influence the corrosion process of RC structures [2]–[4].

The concerns related to climate change include rising temperatures and increased CO_2 concentrations, as well as potential increases in humidity due to heightened precipitation in some regions. These factors collectively elevate the risk of various deterioration processes, including corrosion. Stewart et al. [5], [6] conducted a probabilistic analysis that revealed significant increases in the risks of carbonation-induced and chloride-induced damage for the regions in Australia by the year 2100. To mitigate the effects of a changing climate, the study recommended an increase in the design cover by 10 mm and 5 mm for structures where carbonation and chloride, respectively, compromise durability.

In the work of Saha and Eckelman [7], the impacts of enhanced corrosion on RC structures were examined, specifically focusing on the increased rates of carbonation and chloride diffusion. Their findings suggested that modifications to design codes of concrete [8] structures may be necessary, considering regional climate projections. Notably, in Boston, it was projected that, by 2055 and 2077, the depth of corrosion due to chloride ingress and carbonation, respectively, could surpass the code-mandated protective cover thickness of 38 mm for concrete structures built in the year 2000.

In China, a study made by Peng and Stewart [9] concluded that, by 2100, the mean carbonation depths in RC structures can increase by up to 45% due to climate change. Additionally, climate change can cause an additional 7-20% of carbonation-induced damage in buildings in temperate or cold climate areas in China. Furthermore, Hong et al. [10] concluded that the increase of chloride diffusion from the rising temperatures and relative humidity can result in a reduction of 7 to 19 years in the service life of an RC structure in coastal zones in China. In Malta, Mizzi et al. [11] predict an increase of carbonation depth by up to 40% by 2070 for the worst-case scenario in a similar study.

Orcesi et al. [12] pointed out that it is crucial to acknowledge that climate variables and their effects on concrete are regionally specific, potentially altering the degradation process of building materials and impacting the durability and service life of structures. However, despite the importance of regional climate variables on concrete degradation, relatively few studies have focused on the long-term effects of climate change on structural behavior at the regional level, as shown in Figure 1.

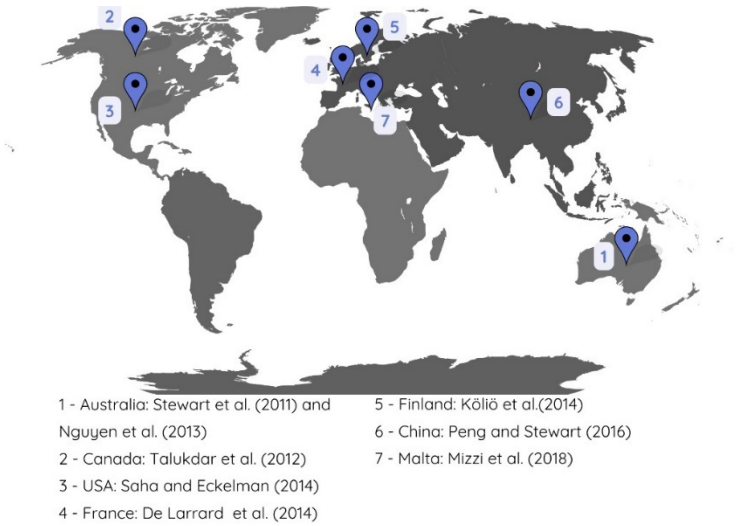

Figure 1. Main articles [3], [7], [9], [11], [13]–[15] conducting a regional analysis of the impact of climate change on the corrosion of RC structures.

These studies collectively highlight the significant impact of climate change on structural durability and performance. Therefore, there is an urgent necessity to investigate the effects of corrosion damage in diverse regions, considering the unique characteristics of reinforced concrete design codes and the prevailing climate conditions specific to each area. Figure 1 accentuates this urgency by revealing a notable gap in knowledge regarding the particular impacts of climate change on structural behavior in Brazil. Consequently, there is a need for more extensive research and analysis in the Brazilian context to comprehensively understand and address these upcoming challenges.

In this work, two dedicated software were developed to emphasize the critical need for addressing this research gap. The first software is utilized to compute the probability of rebar depassivation and crack initiation, considering the rising CO_2 levels projected over time. The second software employs a Finite Element Method based on Positions (FEMP) to determine the probability of failure with respect to the Serviceability Limit State (SLS) of excessive displacement, according to NBR 6118 [16]. This second software integrates laminated frame elements combined with the Mazars damage model [17] for concrete to simulate the behavior of a beam under various configurations during the propagation stage of corrosion. Furthermore, the discussion presented herein encompasses aspects of nonlinear numerical analysis, the consequences of carbonation in the behavior of the structure, and reliability analyses.

2 FINITE ELEMENT METHOD BASED ON POSITIONS USING LAMINATED FRAME ELEMENTS

FEMP is built upon the conventional Finite Element Method (FEM), using positions instead of displacements as nodal variables. This methodology has been applied in several works [18]–[23], each with distinct objectives. This approach employs a total Lagrangian description and the gradient of the change of configuration function is sought. This function describes the transition from an initial fixed configuration to the current configuration in equilibrium. The nodal positions are determined by the principle of minimum total potential energy. As a result, nonlinear equations arise by imposing the nullity of the first variation of the total energy functional, which can be solved using the iterative Newton-Raphson method.

The gradient of the configuration change function is expressed through a composition of the gradient of the mapping from the nondimensional space to the current configuration and the gradient of the inverse of the mapping from the initial configuration to the nondimensional space. These mappings are defined by parametric nondimensional coordinates, which are a function of the initial and current positions of the body.

The mapping function depends on the type of finite element used in the analysis. The approach employed herein involves four degrees of freedom (DOF) for each node, where the first and the second one represent positions in the 2D Cartesian coordinate system, and the third and fourth DOF represent rotation and variation of thickness that is expressed by generalized vectors [18], [20], [24]. The mappings are established by interpolating the position and generalized vectors along a reference line. Also, this numerical model employs the Green-Lagrange strain along with the Saint-Venant-Kirchhoff constitutive model, naturally considering large displacements, as it is objective.

The homogeneous frame element can be utilized to simulate RC structures by considering an equivalent area and inertia. An alternative approach is to employ composite material theories. These materials are classified into fibrous, laminated, particulate composite materials, or a combination of these types [25]. For instance, reinforced steel bars embedded in concrete serve as an example of fiber-reinforced composites, typically formed in the shape of a thin layer known as a lamina [26]. Two main approaches are commonly employed in the kinematics of laminates: the Equivalent Single Layer (ESL) theory and discrete-layer theories [27], [28]. The First-Order Shear Deformation Theory (FSDT), which is categorized into the ESL theory, exhibits a favorable balance between computational efficiency and accuracy when analyzing the global structural behavior of thin and moderately thick composites [29]. To further enhance this theory, the present study incorporated into the FSDT a specific kinematic approach to introduce the zig-zag effect as described in the work of Coda et al. [21].

To represent the material nonlinearity of the concrete, the Mazars damage model [17] was coupled in the numerical software along with the consideration of the perfect plasticity of the steel rebar. For specific details on the formulation, the reader is referenced to Teodoro and Carrazedo [30].

3 CORROSION DUE TO CARBONATION

The corrosion of steel rebars can be defined as an electrochemical process that involves the anodic dissolution of iron and the cathodic reduction of oxygen, with the concrete pores acting as the electrolyte. This process in RC structures is influenced by aggressive agents, like carbon dioxide (CO_2) and chloride ions (Cl^-) [2]. The alkaline nature of the concrete provides passivation for embedded reinforcing rebars, but this passivation of steel is broken down by the presence of Cl^- ions or by the reduction in alkalinity of concrete due to carbonation [31].

The types of corrosion exhibit distinct characteristics, primarily in terms of morphology. Carbonation leads to a relatively uniform corrosion front, affecting the entire extent of the rebars. In contrast, chloride-induced corrosion is localized and manifests as pits [32]. While uniform corrosion may result in a greater overall loss of rebar area, pitting corrosion is more concerning as it causes a greater localized reduction in the cross-sectional area [33].

According to Stefanoni et al. [34], the degradation of RC structures caused by carbonation is becoming increasingly noteworthy because the structures built before modern standards are aging and must be maintained. Besides, the reduction of clinker in cement, undertaken to minimize environmental impact, contributes to a decrease in the pH of concrete, making RC structures more vulnerable to corrosion. Also, the carbonation of concrete has been attracting more attention recently as a result of climate change [35].

Corrosion due to carbonation occurs when CO_2, which penetrates the concrete mainly from absorption and diffusion, reacts with the cement hydration products in concrete, such as calcium hydroxide ($Ca(OH)_2$), resulting in calcium carbonate $CaCO_3$ and water. The formation of $CaCO_3$ decreases the alkalinity in the pores around the rebar [33]. When combined with favorable temperatures, these reactions can disrupt the chemical stability of the passive layer, leading to depassivation of the rebar [2]. This type of corrosion is common in industrial and urban areas where the concentration of CO_2 is high.

Through the corrosion process, two distinct stages can be identified: initiation and propagation [36].

3.1 Initiation

The initiation phase for carbonation is linked to the carbonation depth, which represents the depth to which aggressive agents penetrate the concrete. Once this depth reaches the rebar, the initiation stage is considered complete. This phase is characterized by processes such as the ingress of CO_2, decalcification of the concrete, pH reduction in the porous zone, and depassivation [2].

The progression of the carbonation front is influenced by numerous variables, including concrete compressive strength, CO_2 concentration, temperature, humidity, cement composition, W/C ratio, CO_2 diffusivity, among others [31], [32], [37]. Predicting the time it takes for the carbonation front to reach the rebars is subject to uncertainties, and various models have been proposed in the literature. The initial studies on the relationship between time (t) and carbonation depth (x_c) involved a simplification of Fick's first law:

$$x_c = A\sqrt{t} \tag{1}$$

where A is a constant dependent on CO_2 diffusivity, gradient of CO_2 concentration, and retained quantity of CO_2 in mm/year, according to [33].

Several authors have compared carbonation initiation models in the literature (e.g., [38]–[40]). In the work of Carmona [41], it was concluded that the models proposed by Papadakis et al. [31] and CEB [42] yielded results close to reality, with the CEB [42] model being more generic and easier to apply. These models are found in their original, adapted, or simplified form in many works, such as Sudret [43], [44] and Na et al. [45].

However, in the context of climate change, the equation by Yoon et al. [35] or its derivatives are predominantly employed for calculating carbonation depth in the literature [9], [13], [46], as they account for environmental influences, including time-dependent humidity. Yet, Karimi et al. [47] point out a limitation of Yoon et al. [35] model: Yoon's equation does not incorporate time-dependent CO_2 concentration. In response, Stewart et al. [13] introduced Equation 2 to predict carbonation depth (x_c) in cm.

$$x_c(t) = \sqrt{\frac{2D_{CO_2}(t)}{a} k_{urban} C_{CO_2} (t - 1999)} \left(\frac{t_0}{t-1999}\right)^{n_m}, t \geq 2000 \tag{2}$$

In the Equation 2, k_{urban} represents a new factor designed to amplify the influence of urban environments on CO_2 concentrations; the variable $C_{CO_2}(t)$ denotes the time-dependent mass concentration of ambient CO_2 (expressed in 10^{-3} kg/m^3, adopting 1ppm = 0.0019 10^{-3} kg/m^3); $D_{CO_2}(t)$ stands for the CO_2 diffusion coefficient in concrete; the parameter a denotes the CO_2 binding capacity, indicating the quantity of CO_2 gas a required for the complete carbonation of concrete; the variable n_m serves as the adjustment factor for microclimatic conditions associated with

the frequency of wetting and drying cycles. For sheltered outdoor conditions, n_m assumes a value of 0, while for unsheltered outdoor scenarios, it takes a value of 0.12.

Taking into consideration the study into sheltered outdoor conditions and using a simplified equation similar to Equation 2, this study employs the simplified CEB model [42] used in Sudret [43], [44], in which the carbonation depth in meters is expressed as:

$$x_c(t) = \sqrt{\frac{2D_{CO_2}C_{CO_2}}{a}t} \tag{3}$$

where t is the time (s), C_{CO_2} is the concentration of CO_2 (kg/m^3), D_{CO_2} is the coefficient of diffusion of carbon dioxide in dry concrete (m^2/s) and a is the binding capacity (kg/m^3), and the mean values of each parameter will be discussed in the subsequent sections focusing on its application. This model presented in Equation 3 simplifies the calculation while still maintaining relevance to the underlying physical processes. By utilizing this simplified equation, we aim to provide a comprehensive yet practical assessment of carbonation depth that aligns with current standards and effectively captures the variability and uncertainty inherent in the carbonation process.

3.2 Propagation

The propagation stage begins once depassivation occurs and persists until structural retirement or significant degradation. During this stage, detrimental impacts manifest on both concrete and steel. This includes the generation of corrosion products with larger volumes than the original steel, consequently leading to the development of cracks in the concrete. Moreover, rebar cross section is reduced, the bond strength between the concrete and steel weakens, and the stress at which the rebars yield lowers. In the absence of maintenance, the structure experiences a loss of stiffness and progressively undergoes deformation until structural retirement or significant failure [2], [31], [48].

Herein, the only consequences of corrosion considered are the reduction of rebar cross-section and cracking of the concrete, as described in the following sections. The decrease in steel yield strength and ultimate stress are directly correlated with the corresponding rebar mass loss, as shown by Apostolopoulos and Papadakis [1] through their experimental investigations. The loss of bond strength between concrete and steel is not considered in this study.

3.2.1 Reduction of rebar cross-section area

After depassivation, corrosion leads to chemical and mechanical degradation of the rebars, resulting in the loss of the rebar cross-section. The rate at which this degradation occurs is quantified by means of a corrosion rate (i_{corr}) typically expressed in electrochemical units, i.e., in μA/cm^2 or in mA/m^2. Empirical models are available to estimate i_{corr}, which can either be assumed constant or time-dependent. Various studies provide a review of different models from the literature on i_{corr} (e.g. [40], [49], [50]).

Based on Faraday's law and the density of the material, Val and Melchers [51] and Andrade and Alonso [52] employed a correlation between i_{corr} (in μA/cm^2) and the loss of steel V_{corr} (mm/year), as follows in Equation 4, for uniform corrosion.

$$V_{corr}\left(\frac{mm}{year}\right) = 0.0116\, i_{corr}\left(\frac{\mu A}{cm^2}\right) \tag{4}$$

From this relation of corrosion, many authors, such as Andrade et al. [53] and Val et al. [51], [54], Bastidas-Arteaga et al. [46] and Liberati et al. [55], used Equation 5 to determine the steel bar diameter at a given time (T), which can then be used to calculate the loss of cross-section:

$$\phi(T) = \phi_0 - 0.0232 \int_{T_0}^{T} i_{corr}(t)dt \tag{5}$$

where $\phi(T)$ is the diameter of the rebar under corrosion from time T_0 to T (in years) and ϕ_0 is the initial diameter at time T_0, both in mm.

Other studies proposed different equations to describe the reduction in diameter over time, for either chloride-induced corrosion or due carbonation. For instance, Kiani and Shodja [56] and Biondini and Vergani [57] have proposed distinct relationships in this regard. In this study, the reduction in diameter over time was calculated using Equation 5, since it is based on Faraday's law, offering a simpler, yet effective, approach for calculating the reduction in diameter over time due to corrosion.

3.2.2 Cracking initiation due to corrosion

The reduction in the cross-sectional area of the rebar is associated with the generation of corrosion products, which causes internal pressure in the concrete, inducing tensile stress in the concrete cover. Once the stress reaches the tensile strength of concrete, cracks will start to form [58].

According to Al-Harthy et al. [59], the model for predicting the initiation and propagation of cracks can be influenced by parameters such as the i_{corr}, rebar diameter, concrete cover, and concrete properties. Based on their experimental results, the study concluded that the time span for initial cracking and the propagation period increases with the cover depth and with the reduction in concrete compression strength and rebar diameter. Although the effect of rebar diameter on cracking initiation is a subject of discussion, Al-Harthy et al. [59] and Cui and Alipour [60] pointed out that experimental tests show that lower diameters result in a longer time until cracking begins.

Several equations have been proposed to calculate the time between the depassivation and the beginning of cracking, including equations proposed by Alonso et al. [61], Vidal et al. [62] and El Maaddawy and Soudki [63]. In this work, the time for cracking initiation, after depassivation, (t_{cr}) is calculated using the Equation 8 proposed by Alonso et al. [61], which depends on the diameter of the rebars ($\emptyset$), concrete cover (c) and i_{corr}. In the Equation 6, the term 10^3 is a conversion factor from mm to μm

$$t_{cr} = \frac{7.53+\frac{9.32\,c}{\emptyset}}{0.0116 i_{corr}\times 10^3} \tag{6}$$

4 MONTE CARLO SIMULATION

Due to the uncertainties associated with climate change, loading intensity, types of concrete, and design parameters, a reliability assessment is needed. Reliability can be defined as the complement of the failure probability, i.e., the probability that a system does not fail within a given design life and under specified design and operating conditions [64]. Herein, the term failure does not necessarily imply structural collapse, but rather any undesirable behavior of the structure. In structural reliability, the main challenge lies in incorporating uncertainties into a model that reflects the complex behavior of real-world structures under various conditions. Parameters that are crucial for the model are no longer considered deterministic; they are represented as random variables because uncertainties are introduced through statistical data.

As the exact failure probability in most cases cannot be assessed analytically, transformation methods can be used, such as the First-Order Reliability Method (FORM) or the Second-Order Reliability Method (SORM) [51], [64]. However, while these transformation methods can handle nonlinear limit state functions, they may not be suitable when applied to highly nonlinear problems, such as those involving the structural response to corrosion for the analysis of serviceability limit states and ultimate limit states. Furthermore, when analyzing combined limit states, such as depassivation and crack initiation due to corrosion, the complexity increases due to the potential interdependence between these limit states. As a result, transformation methods may not be the most suitable.

To address these complexities, Monte Carlo Simulation (MCS) is often employed to couple the initiation and propagation phases of corrosion. This approach enables predicting the service life of structures subjected to corrosion, as demonstrated by Liberati et al. [55], Na et al. [45], Stewart et al. [5]. The fundamental equation used to describe failure in this context is based on an indicator function, $I(t)$, where t is discretized time indicating whether failure has occurred at a given time step, if $I(t) = 1$, failure has occurred at time t; if $I(t) = 0$, no failure has occurred. The failure probability, P_f is then derived as:

$$P_f = \frac{1}{N}\sum_{i=1}^{N} I_i(t) \tag{7}$$

where N is the number of Monte Carlo samples, and $I_i(t)$ represents the failure indicator for each sample.

This technique involves generating random samples to artificially simulate a large number of experimental scenarios and observe the outcomes [64]. A numerical model is then evaluated multiple times to produce a set of results that approximate the behavior of the mechanical model, similar to conducting laboratory experiments. These experiments can be schematized according to the following steps: generation of random samples, evaluation of failure occurrence, and estimation of failure and its variance [64].

There are numerous studies available for structures undergoing corrosive processes due to carbonation, each considering different random variables [15], [43], [44], [51], [54], [65]–[68]. These variations arise from the focus on different phases of corrosion, such as initiation [15], [43], [44], [65], [67], [68] or propagation [43], [44], [51], [54], [65]–[67], the limit states being analyzed — such as depassivation, serviceability or ultimate limit states — and the equations used to assess the impact of corrosion on structural performance. Depending on the study's objectives, certain variables may be prioritized, such as rebar diameter or corrosion rate for propagation and diffusivity or concrete cover for initiation.

5 PROBABILITY OF FAILURE

The software utilized in this study was developed to calculate the probabilities of failure related to three distinct limit states: depassivation, crack initiation, and excessive displacement for the Serviceability Limit State (SLS). Subsequent sections will delve into the specific limit state equation for each case, followed by the presentation of results and ensuing discussions.

5.1 Probability of depassivation and crack initiation

As mentioned earlier, depassivation occurs when the carbonation depth reaches the surface of the reinforcement. The calculation for the carbonation depth was performed using Equation 8. The limit state equation for depassivation is defined as follows:

$$g_1(\boldsymbol{x}) = c - \sqrt{\frac{2C_0 D_{CO_2}}{a} t} \tag{8}$$

The random variables were selected in accordance with Table 1. Calculations were conducted considering three distinct mean values for the concrete cover (Cases A, B, and C), each associated with the three environmental aggressiveness classes outlined in NBR 6118 [16]. These classes, designated as A, B, and C, correspond to rural, urban, and industrial areas, respectively, in the Brazilian standard. A similar methodology is outlined in the National House Building Council (NHPC) standards in the UK (2024), where the minimum cover is 25 mm for structures protected or under internal conditions, and 50 mm for those exposed to external conditions.

The value in Table 1 for the concentration of CO_2 was extracted from Félix and Carrazedo [67] and concern to the Brazilian urban environment; diffusivity was based on Sudret [43] in line with studies by Sanjuán and Del Olmo [69] which state that, for medium-quality concrete, CO_2 diffusivity ranges from 5×10^{-8} to 5×10^{-7} m^2/s; for the binding capacity a, the basis was the work of Sudret [43]; and for concrete cover, the basis was the nominal values given by NBR 6118 [16] for environmental aggressiveness classes I, II, and III.

Table 1. Random variables adopted for the initiation stage

Variable	Unit	Reference	Mean value	Coefficient of variation	Distribution
Concentration of CO_2 (C_0)	kg/m^3	Félix e Carrazedo [67]	0.000762	0.1049	Normal
Diffusion of carbon dioxide (D_{CO_2})	m^2/s	Sudret [43]	5×10^{-8}	0.3000	Lognormal
Binding capacity (a)	kg/m^3	Sudret [43]	80.0	0.3000	Lognormal
Concrete cover (c)	cm	NBR 6118 [16], Felix and Carrazedo [67]	2.5 (Case A)	0.1000	Normal
			3.0 (Case B)	0.1000	Normal
			4.0 (Case C)	0.1000	Normal

For a refined analysis, it is essential to account for the increasing concentration of CO_2 over time. Bastidas-Arteaga et al. [46] and Peng and Stewart [65], using the Model for Assessment of Greenhouse-gas Induced Climate

Change, projected CO_2 concentration for various global scenarios. Figure 2 illustrates two projected scenarios: A1F1, which assumes accelerated economic growth, stabilization of population growth by mid-century, introduction of clean and sustainable technologies, and incorporation of fossil energy sources; and A1B, which holds the same premises but adopts a balance between the consumption of fossil and non-fossil energy sources. The projections for low, medium, and high CO_2 concentrations encompass the confidence bounds, which consider both predictive model inaccuracies and the inherent variabilities in CO_2 emissions. It is also shown in this figure the projection resembling the average urban concentration in Brazil reported in Félix and Carrazedo [67], considering that 1 ppm is equivalent to 0.00188×10^{-3} kg/m^3. This comparison with the data in Brazil for 2021 demonstrates that the projection aligns closely with the reference. Afterward, projection scenarios show possible future outcomes whether non-fossil energy sources were incorporated.

Based on the data presented in Figure 2, polynomial regression analysis was conducted to estimate the CO_2 concentration for the medium case scenarios of A1B (Equation 9) and A1FI (Equation 10). The resulting regression models yielded R^2 of 0.99748 and 0.99927 for each curve, respectively.

$$C_0^{A1B}(ppm) = 10039.976 - 12.902t + 0.00403t^2\,;R^2 = 0.99748 \tag{9}$$

$$C_0^{A1F1}(ppm) = 177096.122\ - 178.566t + 0.0451t^2\,;R^2 = 0.99927 \tag{10}$$

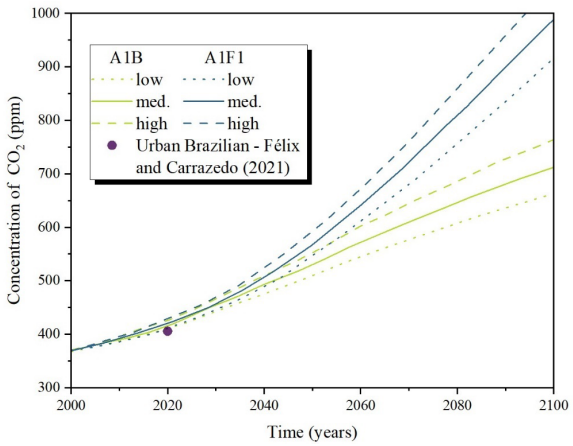

Figure 2. Projection of CO2 concentration for various global scenarios

For the calculation of the depassivation probability over the years, a mean value for CO_2 concentration was computed at each time step according to Equations 9 and 10, while keeping the coefficient of variation from Table 1, as shown in the algorithm in Figure 3. The depassivation probability values over 50 years are presented in Figure 4 for the A1B and A1F1 scenarios, as well as for the constant CO_2, where time $t = 0$ would correspond to the year 2023. A total of 10^6 samples were used.

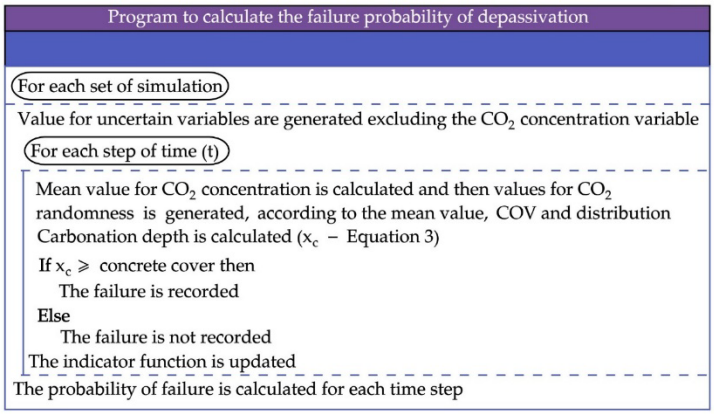

Figure 3. Algorithm to calculate the probability of depassivation

Figure 4 shows that the concrete cover has a fundamental role in the probability of depassivation. In the scenario of constant CO_2 content over the years, the probability of depassivation decreases significantly with the increase in concrete cover, as also shown in Table 2. Furthermore, the increase in CO_2 concentration can lead to earlier depassivation, making it more susceptible to significant damage. As shown in Table 3, 50% of failure probability for concrete cover C exceeds 12 years earlier in A1B scenario compared to constant CO_2 levels.

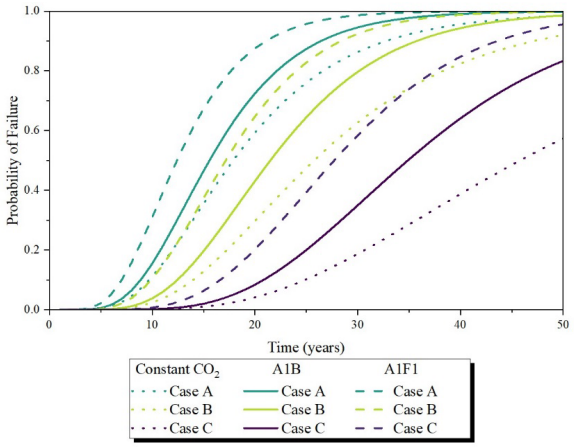

Figure 4. Probability of depassivation over the years considering various carbon dioxide concentration scenarios and different cases of concrete cover (A, B, C)

Table 2. Depassivation probability over the years for three mean coverings assuming constant CO_2

Concrete cover	Time (years)				
	10	**20**	**30**	**40**	**50**
Case A (2.5 cm)	11.081%	59.342%	86.337%	95.626%	98.555%
Case B (3.0 cm)	2.372%	29.678%	62.657%	82.435%	92.031%
Caso C (4.0 cm)	0.076%	4.111%	18.672%	38.754%	57.378%

Table 3. Period in years during which the structure reaches a failure probability greater than 50% for different scenarios

Concrete cover	Scenario (in years)		
	A1B	**A1F1**	**Constant CO_2**
Case A (2.5 cm)	**16**	**13**	**18**
Case B (3.0 cm)	22	18	26
Caso C (4.0 cm)	35	28	42

Once depassivation occurs, the onset of cracking increases the structure's susceptibility to aggressive agents. The time required to initiate cracking can be calculated in various ways, as presented in Section 3.2.2.

For the limit state equation, Equation 6 can be written in the form of Equation 11, utilizing Equation 5 for diameter reduction and assuming i_{corr} is independent of time:

$$\Delta\emptyset(T) = 0.0232 i_{corr} T \Rightarrow \frac{\Delta\emptyset(T)}{2} 10^3 = 7.53 + \frac{9.32c}{\emptyset} \tag{11}$$

From Equation 11, we define the limit state equation to find the time for crack initiation:

$$g_2(\boldsymbol{x}) = -\frac{\Delta\emptyset(T).10^3}{2} + \left(7{,}53 + \frac{9{,}32c}{\emptyset_0}\right) \tag{12}$$

Since the calculation of initiation time and corroded bar diameter are based on random variables, they become random variables themselves, as shown in the algorithm in Figure 5. The values of c, C_{CO_2}, D_{CO_2}, and a for the initiation time calculation and $\emptyset(T)$ are the same as in Table 1. The statistic distribution for the corrosion rate i_{corr} adopted in this study is listed in Table 4.

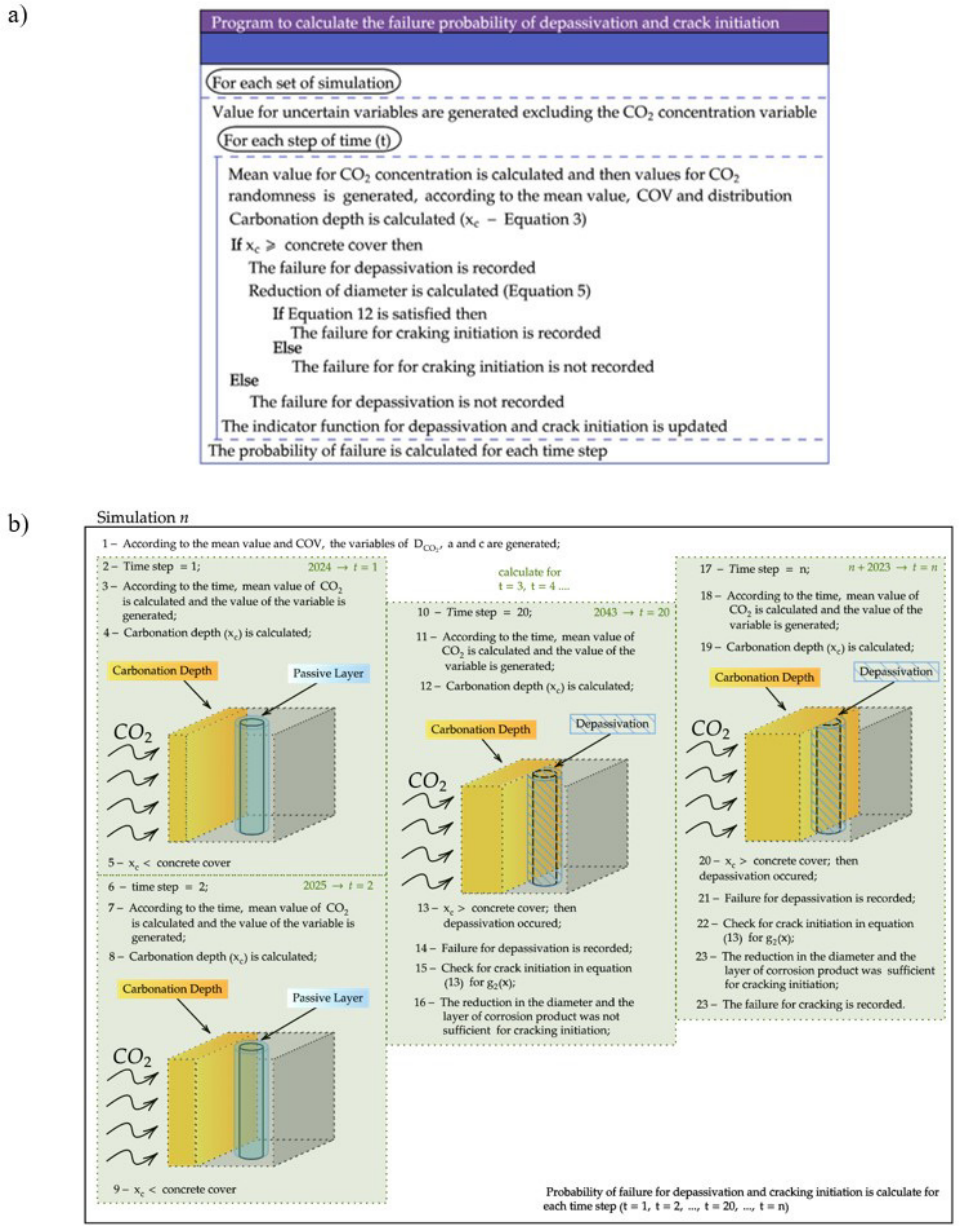

Figure 5. Algorithm to calculate the probability of crack initiation

To observe the influence of rebar diameter three diameters (5, 10, and 20 mm) values were adopted along with a concrete cover of 3 cm. The cracking probability over the next 50 years is presented in Figure 6, where "Initiation" represents the depassivation probability, and time $t = 0$ corresponds to the year 2023.

Based on the results obtained from the various scenarios regarding cracking over the years, it can be stated that the structure's service life may be shortened under the presented conditions. Within 50 years, depassivation is observed, followed by initiation of cracks, making the structure more vulnerable to aggressive agents. These findings once again underscore the importance of the concrete cover, extending the structure's service life if chosen and executed correctly.

The choice of steel diameter used in the structure also significantly influences cracking. Looking solely at the cracking results and considering that a reinforced concrete beam may have all three types of diameters, say, 5 mm in stirrups, 20 mm in tension reinforcement, and 10 mm in compression, cracking may primarily occur in the tension reinforcement.

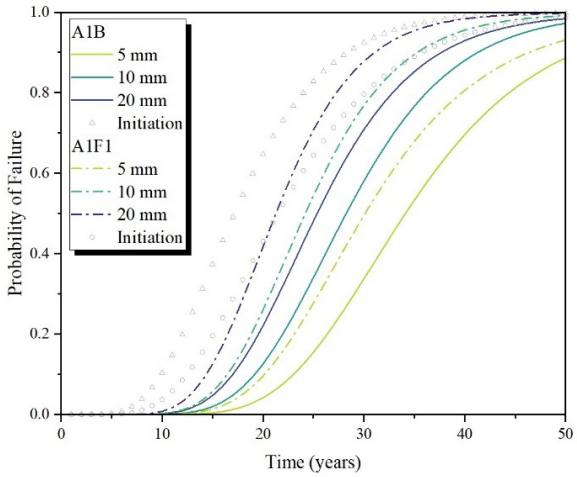

Figure 6. Cracking probability over the years for different scenarios

5.2 Propagation Failure due to excessive displacement – Serviceability Limit State

According to NBR 6118 [16], a concrete structure must be evaluated for SLS, including excessive displacement, crack formation, crack width, excessive vibration, among others. These limits are related to the structure's durability, user comfort, appearance, and proper utilization of the structures.

In this study, only the SLS concerning displacement within the sensory acceptability (user comfort) is evaluated, meaning that the permissible deflection for the structure (RC beam) is $\ell/250$, where ℓ is the span length. It is understood that reaching this limit may or may not imply that the structure has reached other serviceability limit states, but only excessive displacement was considered herein.

Thus, the limit state equation for failure in the propagation stage due to the excessive deflection is defined as follows:

$$g_3(\boldsymbol{x}) = \frac{\ell}{250} - y(t, midspan) \tag{13}$$

where $\mathrm{y(t, midspan)}$ is the midspan deflection at time step t.

The choice of variables depends on the specific case under study. In this study, the failure probability of the beam from the work by Álvares [71], shown in Figure 7, was calculated, considering the variables listed in Table 4. The dead load variability follows [70]. However, recent studies have addressed the temporal and spatial variability of live loads in buildings in Brazil. For further insight into the consideration of other types of loads in Brazil, readers can refer to the work of Costa et al. [72]. Besides, it can be noticed that no stirrups were considered in the calculation. Concrete covers were chosen to include the required values by NBR 6118 [16]. The calculation was performed at six time steps: 0, 15, 30, 45, 60, and 75 years. These intervals represent the propagation period, assuming that depassivation has already occurred. A time span exceeding 50 years was included as the structure's failure time is expected to be longer. The algorithm used, which calculates the beam deflection through the FEMP numerical software presented in Section 2, as well as the failure probability, is shown in Figure 8. The numerical model, including the validation of the beam from Álvares [71] in the non-corroded state, is detailed in Teodoro and Carrazedo [30]

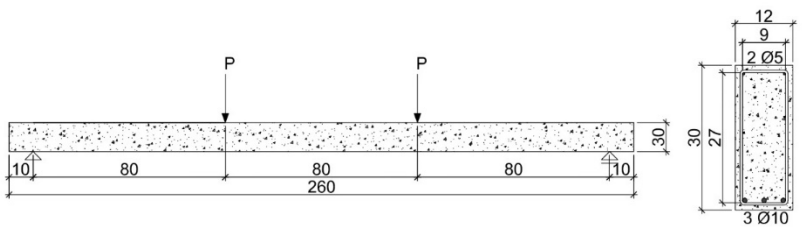

Figure 7. Experimental test configuration of a reinforced concrete beam by Álvares [71]. Dimensions in cm.

Table 4. Random variables for calculating failure probability due to excessive displacement and rebar cross-section reduction

Variables	Unit	Reference	Mean value	Coefficient of variation	Distribution
Corrosion rate (i_{corr})	$\frac{\mu A}{cm^2}$	Peng and Stewart [65]	0.5	1.00	Lognormal
External (dead) load (P)	kN	Coelho [70]	36.0	0.10	Gumbel
Concrete cover (c)	cm	Félix and Carrazedo [67]	3.0	0.12	Normal

One of the characteristics of uniform corrosion, as observed in Equation 5, is that the smaller rebar cross-section is more prone to damage, because $\Delta\phi$ depends on i_{corr}, T and V_{corr} that do not depend on the rebar diameter [73]. Building upon this, the failure probability was calculated for the original experiment, consisting of 3 bars with a diameter of 10 mm, and alternatively, for 12 bars with a diameter of 5 mm, resulting in the same reinforcement area. The probability of failure over time is presented in Figure 9. A total of 10^4 samples were used for the beam with 5 mm bars and 4×10^4 samples for the beam with 10 mm bars to ensure a 95% confidence interval.

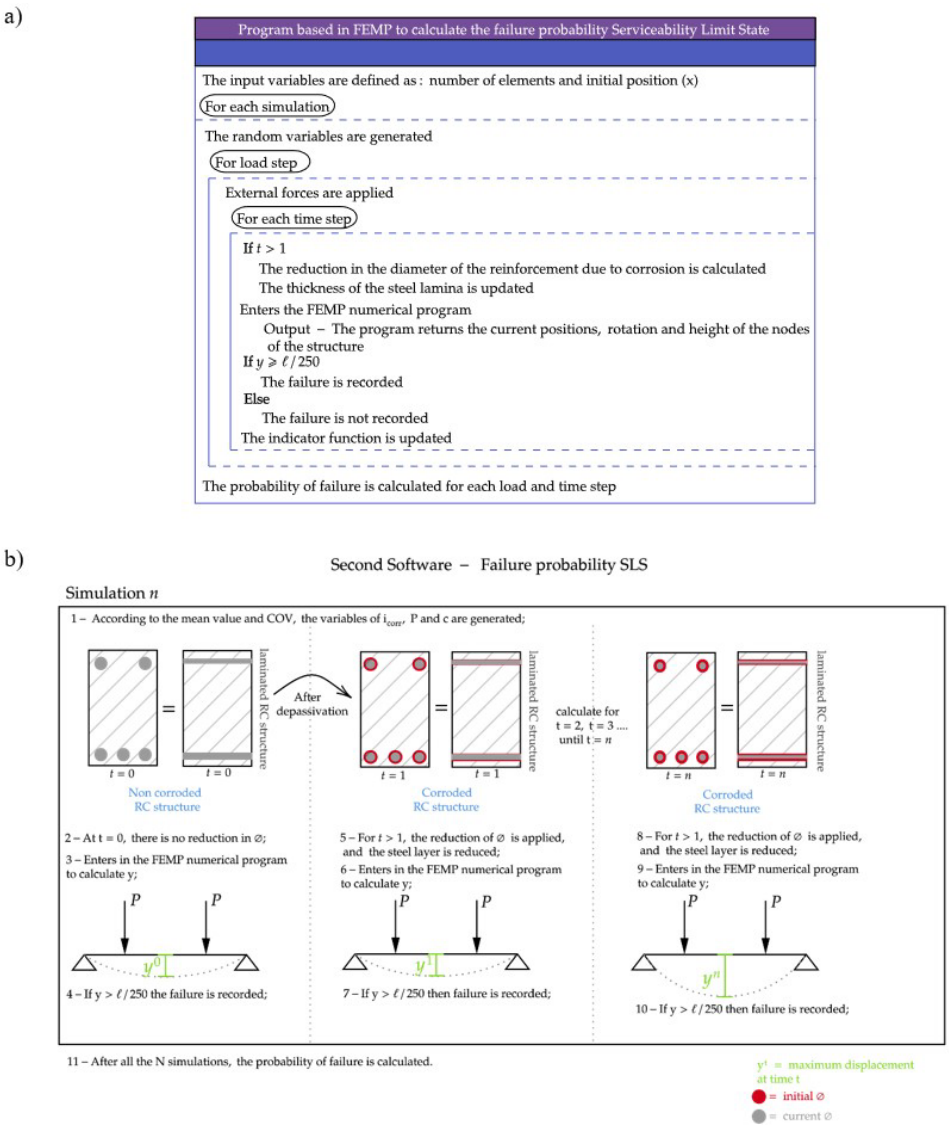

Figure 8. Algorithm to calculate the probability of excessive displacement.

Figure 10 displays the number of failures over time for groups of one hundred samples. This graph provides a clearer understanding of how the failure count progresses, depicting the behavior of the indicator function throughout the SLS.

i. The presented results on flexural failure probability yield several noteworthy conclusions: The choice of reinforcement diameter is a critical consideration in the design, particularly in areas with a high degree of aggressiveness, such as industrial environments where CO_2 levels are elevated;

ii. The results depicted in Figure 9 align with the findings of El Hassan et al. [32], who concluded that the probability of failure for a reinforced concrete bridge beam is higher for structures employing smaller-diameter bars compared to fewer larger-diameter bars. In their case, the probability of failure is three times higher when comparing the use of 9 bars of 20 mm to 6 bars of 25 mm;

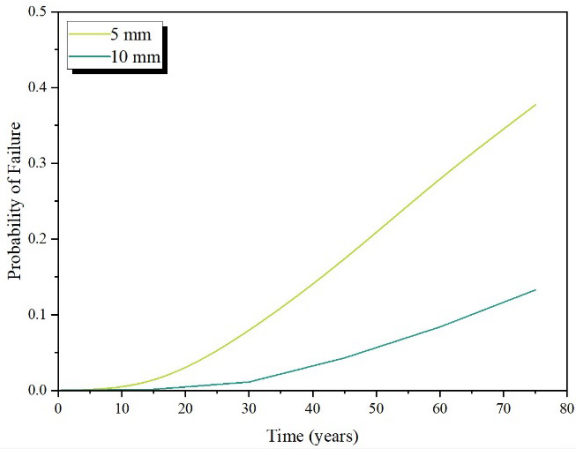

Figure 9. Probability of failure due to excessive displacement over the years for the beam of the work of Álvares [71].

iii. Given that the smaller diameter bar undergoes more significant degradation due to corrosion, the failure mode of the structure might change. As the corrosion progresses, stirrups and compression reinforcement may lose their structural function, while flexural reinforcement, typically of a larger diameter, can continue to function at an acceptable level.

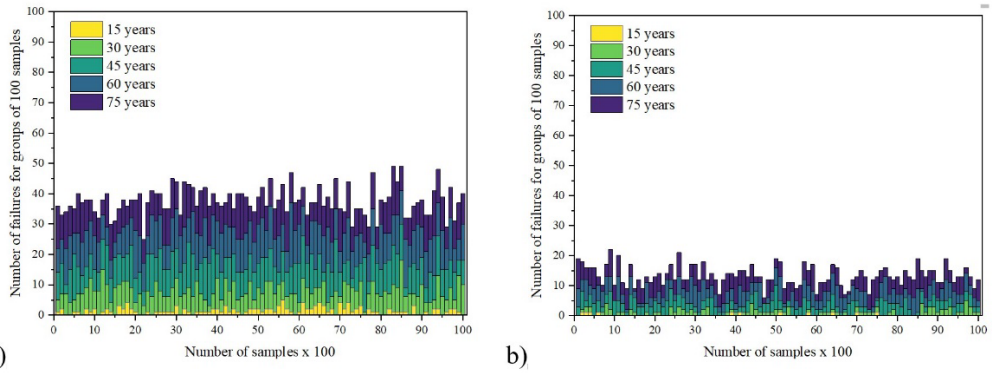

Figure 10. Mapping the number of failures per hundred samples over 15 to 75 years for diameters of a) 5 mm and b) 10 mm.

6 DISCUSSION

The results obtained in Section 5 highlighted the significant influence of the concrete cover depth on depassivation and the cracking initiation due to corrosion. However, in construction in Brazil, there is often a lack of compliance with the required concrete cover depth. This non-compliance can lead to an earlier onset of corrosion, which in turn can result in structural issues such as cracking and loss of stiffness.

Additionally, the reinforcement diameter presents conflicting effects: while smaller diameter delays cracking initiation, it concurrently shortens the failure time concerning excessive displacement. Since failure time due to excessive displacement is concerning and may indicate a closer approach to structural collapse, this aspect requires careful attention.

It's important to highlight that this study did not account for the impact of concrete cracking on structural strength and the accelerated penetration of aggressive agents, which could influence the overall durability and safety of the structure.

In a beam, both longitudinal and transverse reinforcements are employed, with the former typically having a larger diameter than the latter. The conventional failure mode associated with beams is flexural failure. However, as steel loss is more severe in smaller diameter bars, the beam may experience rupture in transverse reinforcements, resulting in shear failure. The choice of reinforcement diameter significantly influences the structure's failure mode. While this study did not delve into shear failure, it is strongly recommended for exploration in future research.

In a 50-year timeframe, the structure may experience depassivation, cracking, and failure due to excessive displacement in the SLS. In terms of depassivation, structures in case A are 72% more likely to experience failure within 50 years compared to structures in case C (concrete cover of 4cm), assuming that CO_2 levels remain constant. However, these results worsen when considering scenario A1F1 (fossil-prone usage). For depassivation, the structure of case A reaches a 50% or higher probability within 13 years, whereas case C structures reach this threshold in 28 years, assuming scenario A1F1. This contrasts with 18 and 46 years for cases A and C, respectively, under the constant CO_2 scenario.

Regarding cracking initiation, the likelihood of failure within 50 years increases by 18% when using a 20 mm diameter compared to a 5 mm diameter for case B (concrete cover of 3cm). In contrast, failure due to excessive displacement becomes less likely with larger diameter. Specifically, over 75 years, using a 5 mm diameter results in a failure probability 187% higher than using a 10 mm diameter.

Several variables were not considered in this study, including the loss of bond between steel and concrete, the reduction in concrete strength due to cracking, the decrease in steel yield strength in tandem with steel nonlinearity, among other pertinent factors.

The decision to decouple the problems (initiation and SLS) was based on the need to first establish a clear understanding of the individual effects before combining them. Coupling depassivation and propagation would improve results, but here we focus on the propagation and its effects on the long run.

7 CONCLUSION

Research studies worldwide have increasingly focused on understanding the heightened corrosion resulting from climate change. However, the impact of climate variables on concrete is unique to each region, potentially altering the degradation process of building materials and affecting the durability and service life of structures. It is imperative to conduct a study specifically addressing these effects in the context of Brazil.

In this study, we provided an analysis to anticipate the impacts of corrosion on structures, considering the stage of initiation and propagation. For the analysis of structural failure in the excessive displacement serviceability limit state, the Finite Element Method based on Positions, employing laminated frame elements, was utilized to calculate structural response under corrosion and external loads (dead loads).

The results clearly illustrate that the choice of concrete cover significantly influences the depassivation process, as expected, capable of either prolonging or delaying it. For instance, increasing the concrete cover from 2.5 cm to 3.0 cm leads to a 50% reduction in the probability of depassivation within a 20-year span. Moreover, a rise in CO_2 concentration accelerates the onset of corrosion, with a structure having a 50% probability of depassivation in just 28 years under the A1F1 scenario (fossil-prone usage), compared to the 46 years required under constant CO_2 conditions for case C (concrete cover of 3cm) — a notable reduction of 18 years in the initiation period.

In addition, the diameter of reinforcements displays a dual impact. While a smaller diameter extends the initiation time for cracking, resulting in a 13% reduction in the probability of crack initiation when using a 5 mm diameter instead of 10 mm over a 50-year period, it concurrently diminishes the failure time for the case of excessive displacement. Specifically, opting for a 5 mm diameter increases the probability of failure by 311% within 45 years compared to using a 10 mm diameter, using equivalent reinforcement areas.

A significant concern arises as we project 50 years ahead, anticipating potential depassivation, cracking, and structural failure. This concern is heightened in Brazil, especially in the São Paulo region where initial data was gathered, not only due to the worrisome results of the analysis considering only the increase in CO_2 concentration, but also due to the predicted rise in temperature and humidity in certain regions, which is expected to further exacerbate the situation. Compounding this, many constructions in Brazil do not adhere to the prescribed standards for concrete cover, bringing up a concerning situation for the future. Addressing this multifaceted concern will be a primary focus

of our future research, aiming to develop a more comprehensive understanding of the climate-induced effects on structural durability and performance in different areas of Brazil and combining initiation and propagation.

ACKNOWLEDGEMENTS

This research was funded by the Brazilian National Council for Scientific and Technological Development (CNPq, grant n. 302885/2022-6), the Coordination of Superior Level Staff Improvement–Brasil (CAPES)–Finance Code 001 and grant 2023/13093-9, São Paulo Research Foundation (FAPESP)

REFERENCES

[1] C. A. Apostolopoulos and V. G. Papadakis, "Consequences of steel corrosion on the ductility properties of reinforcement bar," *Constr. Build. Mater.*, vol. 22, no. 12, pp. 2316–2324, Dec 2008, http://doi.org/10.1016/j.conbuildmat.2007.10.006.

[2] R. Rodrigues, S. Gaboreau, J. Gance, I. Ignatiadis, and S. Betelu, "Reinforced concrete structures: a review of corrosion mechanisms and advances in electrical methods for corrosion monitoring," *Constr. Build. Mater.*, vol. 269, pp. 121240, 2021, http://doi.org/10.1016/j.conbuildmat.2020.121240.

[3] A. Köliö, T. A. Pakkala, J. Lahdensivu, and M. Kiviste, "Durability demands related to carbonation induced corrosion for Finnish concrete buildings in changing climate," *Eng. Struct.*, vol. 62–63, pp. 42–52, Mar 2014, http://doi.org/10.1016/j.engstruct.2014.01.032.

[4] E. Bastidas-Arteaga, A. Chateauneuf, M. Sánchez-Silva, P. Bressolette, and F. Schoefs, "Influence of weather and global warming in chloride ingress into concrete: a stochastic approach," *Struct. Saf.*, vol. 32, no. 4, pp. 238–249, Jul 2010, http://doi.org/10.1016/j.strusafe.2010.03.002.

[5] M. G. Stewart, X. Wang, and M. N. Nguyen, "Climate change adaptation for corrosion control of concrete infrastructure," *Struct. Saf.*, vol. 35, pp. 29–39, 2012, http://doi.org/10.1016/j.strusafe.2011.10.002.

[6] M. G. Stewart, X. Wang, and M. N. Nguyen, "Climate change impact and risks of concrete infrastructure deterioration," *Eng. Struct.*, vol. 33, no. 4, pp. 1326–1337, 2011, http://doi.org/10.1016/j.engstruct.2011.01.010.

[7] M. Saha and M. J. Eckelman, "Urban scale mapping of concrete degradation from projected climate change," *Urban Clim.*, vol. 9, pp. 101–114, 2014, http://doi.org/10.1016/j.uclim.2014.07.007.

[8] American Concrete Institute, *ACI Code: Building Code Requirements for Structural Concrete and Commentary*, ACI 318-11, 2011.

[9] L. Peng and M. G. Stewart, "Climate change and corrosion damage risks for reinforced concrete infrastructure in China," *Struct. Infrastruct. Eng.*, vol. 12, no. 4, pp. 499–516, Apr 2016, http://doi.org/10.1080/15732479.2013.858270.

[10] M. Hong, X. Zhao, J. Chen, and T. Xie, "Effect of global warming on chloride resistance of concrete: a case study of Guangzhou, China," in *Adapting the Built Environment for Climate Change*, F. Pacheco-Torgal and C.-G. Granqvist, Eds., Cambridge: Woodhead Publishing, 2023, pp. 201–212. http://doi.org/10.1016/B978-0-323-95336-8.00013-5.

[11] B. Mizzi, Y. Wang, and R. P. Borg, "Effects of climate change on structures: analysis of carbonation-induced corrosion in Reinforced Concrete Structures in Malta," *IOP Conf. Ser. Mater. Sci. Eng.*, vol. 442, pp. 012023, Nov. 2018, http://doi.org/10.1088/1757-899X/442/1/012023.

[12] A. Orcesi et al., "Investigating the effects of climate change on material properties and structural performance," *Struct. Eng. Int.*, vol. 32, no. 4, pp. 577–588, 2022, http://doi.org/10.1080/10168664.2022.2107468.

[13] M. G. Stewart, X. Wang, and M. N. Nguyen, "Climate change impact and risks of concrete infrastructure deterioration," *Eng. Struct.*, vol. 33, no. 4, pp. 1326–1337, 2011, http://doi.org/10.1016/j.engstruct.2011.01.010.

[14] S. Talukdar, N. Banthia, and J. R. Grace, "Carbonation in concrete infrastructure in the context of global climate change - Part 1: Experimental results and model development," *Cement Concr. Compos.*, vol. 34, no. 8, pp. 924–930, Sep 2012, http://doi.org/10.1016/j.cemconcomp.2012.04.011.

[15] T. de Larrard, E. Bastidas-Arteaga, F. Duprat, and F. Schoefs, "Effects of climate variations and global warming on the durability of RC structures subjected to carbonation," *Civ. Eng. Environ. Syst.*, vol. 31, no. 2, pp. 153–164, 2014, http://doi.org/10.1080/10286608.2014.913033.

[16] Associação Brasileira de Normas Técnicas, *Projeto de Estruturas de Concreto – Procedimento*, ABNT NBR 6118, 2023.

[17] J. Mazars and G. Pijaudier-Cabot, "Continuum damage theory: application to concrete," *J. Eng. Mech.*, vol. 115, no. 2, pp. 345–365, 1989. http://doi.org/10.1061/(ASCE)0733-9399(1989)115:2(345).

[18] R. Carrazedo and H. B. Coda, "Triangular based prismatic finite element for the analysis of orthotropic laminated beams, plates and shells," *Compos. Struct.*, vol. 168, pp. 234–246, 2017, http://doi.org/10.1016/j.compstruct.2017.02.027.

[19] H. B. Coda and M. Greco, "A simple FEM formulation for large deflection 2D frame analysis based on position description," *Comput. Methods Appl. Mech. Eng.*, vol. 193, no. 33–35, pp. 3541–3557, Aug 2004, http://doi.org/10.1016/j.cma.2004.01.005.

[20] H. B. Coda and R. R. Paccola, "An alternative positional FEM formulation for geometrically non-linear analysis of shells: Curved triangular isoparametric elements," *Comput. Mech.*, vol. 40, no. 1, pp. 185–200, 2007, http://doi.org/10.1007/s00466-006-0094-1.

[21] H. B. Coda, R. R. Paccola, and R. Carrazedo, "Zig-Zag effect without degrees of freedom in linear and non linear analysis of laminated plates and shells," *Compos. Struct.*, vol. 161, pp. 32–50, 2017, http://doi.org/10.1016/j.compstruct.2016.10.129.

[22] R. Carrazedo and H. B. Coda, "Alternative positional FEM applied to thermomechanical impact of truss structures," *Finite Elem. Anal. Des.*, vol. 46, no. 11, pp. 1008–1016, Nov 2010, http://doi.org/10.1016/j.finel.2010.07.008.

[23] G. Avancini and R. A. K. Sanches, "A total Lagrangian position-based finite element formulation for free-surface incompressible flows," *Finite Elem. Anal. Des.*, vol. 169, pp. 103348, Feb 2020, http://doi.org/10.1016/j.finel.2019.103348.

[24] H. B. Coda and R. R. Paccola, "A positional FEM Formulation for geometrical non-linear analysis of shells," *Lat. Am. J. Solids Struct.*, vol. 5, no. 3, pp. 205–223, 2008.

[25] R. M. Jones, *Mechanics of Composite Materials*, 2nd ed. Philadelphia: Taylor & Francis, 1999, http://doi.org/10.5406/j.ctt1v2xsbz.1.

[26] J. N. Reddy, *Mechanics of Laminated Composite Plates and Shells: Theory and Analysis.* Florida: CRC Press, 2003. http://doi.org/10.1201/b12409.

[27] I. Kreja, "A literature review on computational models for laminated composite and sandwich panels," *Open Eng.*, vol. 1, no. 1, pp. 59–80, 2011, http://doi.org/10.2478/s13531-011-0005-x.

[28] R. Khandan, S. Noroozi, P. Sewell, and J. Vinney, "The development of laminated composite plate theories," *J. Mater. Sci.*, vol. 47, no. 16, pp. 5901–5910, 2012, http://doi.org/10.1007/s10853-012-6329-y.

[29] Y. X. Zhang and C. H. Yang, "Recent developments in finite element analysis for laminated composite plates," *Compos. Struct.*, vol. 88, no. 1, pp. 147–157, Mar 2009, http://doi.org/10.1016/j.compstruct.2008.02.014.

[30] C. P. Teodoro and R. Carrazedo, "Nonlinear numerical analysis of corroded reinforced concrete structures using laminated frame elements," *Mater. Struct.*, vol. 57, no. 5, pp. 109, Jun 2024, http://doi.org/10.1617/s11527-024-02386-y.

[31] V. G. Papadakis, C. G. Vayenas, and M. N. Fardis, "A reaction engineering approach to the problem of concrete carbonation," *AIChE J.*, vol. 35, no. 10, pp. 1639–1650, 1989, http://doi.org/10.1002/aic.690351008.

[32] J. El Hassan, P. Bressolette, A. Chateauneuf, and K. El Tawil, "Reliability-based assessment of the effect of climatic conditions on the corrosion of RC structures subject to chloride ingress," *Eng. Struct.*, vol. 32, no. 10, pp. 3279–3287, Oct 2010, http://doi.org/10.1016/j.engstruct.2010.07.001.

[33] L. Basheer, J. Kropp, and D. J. Cleland, "Assessment of the durability of concrete from its permeation properties: a review," *Constr. Build. Mater.*, vol. 15, no. 2–3, pp. 93–103, 2001, http://doi.org/10.1016/S0950-0618(00)00058-1.

[34] M. Stefanoni, U. Angst, and B. Elsener, "Corrosion rate of carbon steel in carbonated concrete: a critical review," *Cement Concr. Res.*, vol. 103, pp. 35–48, 2018, http://doi.org/10.1016/j.cemconres.2017.10.007.

[35] I. S. Yoon, O. Çopuroğlu, and K. B. Park, "Effect of global climatic change on carbonation progress of concrete," *Atmos. Environ.*, vol. 41, no. 34, pp. 7274–7285, Nov 2007, http://doi.org/10.1016/j.atmosenv.2007.05.028.

[36] K. Tuutti, *Corrosion of Steel in Concrete.* Stockholm: Swedish Cement and Concrete Research, 1982.

[37] A. V. Saetta and R. V. Vitaliani, "Experimental investigation and numerical modeling of carbonation process in reinforced concrete structures: part I: theoretical formulation," *Cement Concr. Res.*, vol. 34, no. 4, pp. 571–579, Apr 2004, http://doi.org/10.1016/j.cemconres.2003.09.009.

[38] S. H. Han, W. S. Park, and E. I. Yang, "Evaluation of concrete durability due to carbonation in harbor concrete structures," *Constr. Build. Mater.*, vol. 48, pp. 1045–1049, 2013, http://doi.org/10.1016/j.conbuildmat.2013.07.057.

[39] Y. Zhou, B. Gencturk, K. Willam, and A. Attar, "Carbonation-induced and chloride-induced corrosion in reinforced concrete structures," *J. Mater. Civ. Eng.*, vol. 27, no. 9, pp. 04014245, 2015, http://doi.org/10.1061/(ASCE)MT.1943-5533.0001209.

[40] B. Sun, R. Xiao, W. Ruan, and P. Wang, "Corrosion-induced cracking fragility of RC bridge with improved concrete carbonation and steel reinforcement corrosion models," *Eng. Struct.*, vol. 208, pp. 110313, 2020, http://doi.org/10.1016/j.engstruct.2020.110313.

[41] T. Carmona, “Modelos de previsão da despassivação das armaduras em estruturas de concreto sujeitas à carbonatação,” M.S. thesis, Univ. São Paulo, São Paulo, 2005. http://doi.org/10.11606/D.3.2005.tde-27072005-163131.

[42] International Federation for Structural Concrete, *New Approach to Durability Design: an Example for Carbonation Induced Corrosion*, 1997.

[43] B. Sudret, "Probabilistic models for the extent of damage in degrading reinforced concrete structures," *Reliab. Eng. Syst. Saf.*, vol. 93, no. 3, pp. 410–422, 2008, http://doi.org/10.1016/j.ress.2006.12.019.

[44] B. Sudret, G. Defaux, and M. Pendola, "Stochastic evaluation of the damage length in RC beams submitted to corrosion of reinforcing steel," *Civ. Eng. Environ. Syst.*, vol. 24, no. 2, pp. 165–178, 2007, http://doi.org/10.1080/10286600601159305.

[45] U. J. Na, S. J. Kwon, S. R. Chaudhuri, and M. Shinozuka, "Stochastic model for service life prediction of RC structures exposed to carbonation using random field simulation," *KSCE J. Civ. Eng.*, vol. 16, no. 1, pp. 133–143, 2012, http://doi.org/10.1007/s12205-012-1248-7.

[46] E. Bastidas-Arteaga, F. Schoefs, M. G. Stewart, and X. Wang, "Influence of global warming on durability of corroding RC structures: A probabilistic approach," *Eng. Struct.*, vol. 51, pp. 259–266, 2013, http://doi.org/10.1016/j.engstruct.2013.01.006.

[47] A. Karimi, M. Ghanooni-Bagha, E. Ramezani, A. A. Shirzadi Javid, and M. Zabihi Samani, "Influential factors on concrete carbonation: a review," *Mag. Concr. Res.*, vol. 75, no. 23, pp. 1212–1242, May 2023, http://doi.org/10.1680/jmacr.22.00252.

[48] W. Zhu and R. François, "Experimental investigation of the relationships between residual cross-section shapes and the ductility of corroded bars," *Constr. Build. Mater.*, vol. 69, pp. 335–345, Oct 2014, http://doi.org/10.1016/j.conbuildmat.2014.07.059.

[49] M. Raupach, "Models for the propagation phase of reinforcement corrosion: an overview," *Mater. Corros.*, vol. 57, no. 8, pp. 605–613, Aug 2006, http://doi.org/10.1002/maco.200603991.

[50] M. B. Otieno, H. D. Beushausen, and M. G. Alexander, "Modelling corrosion propagation in reinforced concrete structures - A critical review," *Cement Concr. Compos.*, vol. 33, no. 2, pp. 240–245, Feb 2011, http://doi.org/10.1016/j.cemconcomp.2010.11.002.

[51] D. V. Val and R. E. Melchers, "Reliability of deteriorating RC slab bridges," *J. Struct. Eng.*, vol. 123, no. 12, pp. 1638–1644, 1997, http://doi.org/10.1061/(ASCE)0733-9445(1997)123:12(1638).

[52] C. Andrade and C. Alonso, "Test methods for on-site corrosion rate measurement of steel reinforcement in concrete by means of the polarization resistance method," *Mater. Struct.*, vol. 37, no. 273, pp. 623–643, 2004, http://doi.org/10.1007/BF02483292.

[53] C. Andrade, C. Alonso, and F. J. Molina, "Cover cracking as a function of bar corrosion: part I-experimental test," *Mater. Struct.*, vol. 26, no. 8, pp. 453–464, 1993, http://doi.org/10.1007/BF02472805.

[54] D. V. Val, M. G. Stewart, and R. E. Melchers, "Effect of reinforcement corrosion on reliability of highway bridges," *Eng. Struct.*, vol. 20, no. 11, pp. 1010–1019, 1998, http://doi.org/10.1016/S0141-0296(97)00197-1.

[55] E. A. P. Liberati, E. D. Leonel, and C. G. Nogueira, "Influence of the reinforcement corrosion on the bending moment capacity of reinforced concrete beams: a structural reliability approach," *Rev. IBRACON Estrut. Mater.*, vol. 7, no. 3, pp. 379–413, 2014, http://doi.org/10.1590/S1983-41952014000300005.

[56] K. Kiani and H. M. Shodja, "Prediction of the penetrated rust into the microcracks of concrete caused by reinforcement corrosion," *Appl. Math. Model.*, vol. 35, no. 5, pp. 2529–2543, 2011, http://doi.org/10.1016/j.apm.2010.11.039.

[57] F. Biondini and M. Vergani, "Deteriorating beam finite element for nonlinear analysis of concrete structures under corrosion," *Struct. Infrastruct. Eng.*, vol. 11, no. 4, pp. 519–532, Apr 2015, http://doi.org/10.1080/15732479.2014.951863.

[58] E. Chen and C. K. Y. Leung, "Finite element modeling of concrete cover cracking due to non-uniform steel corrosion," *Eng. Fract. Mech.*, vol. 134, pp. 61–78, 2015, http://doi.org/10.1016/j.engfracmech.2014.12.011.

[59] A. S. Al-Harthy, M. G. Stewart, and J. Mullard, "Concrete cover cracking caused by steel reinforcement corrosion," *Mag. Concr. Res.*, vol. 63, no. 9, pp. 655–667, Sep 2011, http://doi.org/10.1680/macr.2011.63.9.655.

[60] Z. Cui and A. Alipour, "Concrete cover cracking and service life prediction of reinforced concrete structures in corrosive environments," *Constr. Build. Mater.*, vol. 159, pp. 652–671, Jan 2018, http://doi.org/10.1016/j.conbuildmat.2017.03.224.

[61] C. Alonso, C. Andrade, J. Rodriguez, and J. M. Diez, "Factors controlling cracking of concrete affected by reinforcement corrosion," *Mater. Struct.*, vol. 31, no. 211, pp. 435–441, 1998, http://doi.org/10.1007/BF02480466.

[62] T. Vidal, A. Castel, and R. François, "Analyzing crack width to predict corrosion in reinforced concrete," *Cement Concr. Res.*, vol. 34, no. 1, pp. 165–174, 2004, http://doi.org/10.1016/S0008-8846(03)00246-1.

[63] T. El Maaddawy and K. Soudki, "A model for prediction of time from corrosion initiation to corrosion cracking," *Cement Concr. Compos.*, vol. 29, no. 3, pp. 168–175, 2007, http://doi.org/10.1016/j.cemconcomp.2006.11.004.

[64] R. E. Melchers and A. T. Beck, *Structural Reliability Analysis and Prediction*, 3rd ed. Hoboken, USA: Wiley, 2018.

[65] J. Peng and M. G. Stewart, *Carbonation-induced Corrosion Damage and Structural Safety for Concrete Structures Under Enhanced Greenhouse Conditions* (Centre for Infrastucture Performance and Reliability - Research Report 270.11.2008). New South Wales: Univ. Newcastle, 2008.

[66] F. Chen, H. Baji, and C. Q. Li, "A comparative study on factors affecting time to cover cracking as a service life indicator," *Constr. Build. Mater.*, vol. 163, pp. 681–694, 2018, http://doi.org/10.1016/j.conbuildmat.2017.12.120.

[67] E. F. Félix and R. Carrazedo, "Análise probabilística da vida útil de lajes de concreto armado sujeitas à corrosão por carbonatação via simulação de Monte Carlo," *Materia*, vol. 26, no. 3, e13043, 2021., http://doi.org/10.1590/s1517-707620210003.13043.

[68] X. Wang, M. G. Stewart, and M. Nguyen, "Impact of climate change on corrosion and damage to concrete infrastructure in Australia," *Clim. Change*, vol. 110, no. 3–4, pp. 941–957, Feb 2012, http://doi.org/10.1007/s10584-011-0124-7.

[69] M. A. Sanjuán and C. Del Olmo, "Carbonation resistance of one industrial mortar used as a concrete coating," *Build. Environ.*, vol. 36, no. 8, pp. 949–953, 2001, http://doi.org/10.1016/S0360-1323(00)00045-7.

[70] K. O. Coelho, “Modelos numéricos aplicados à modelagem probabilística da degradação mecânica do concreto e corrosão de armaduras,” M.S. thesis, Univ. São Paulo, São Carlos, 2017.

[71] M. S. Álvares, “Estudo de um modelo de dano para o concreto: formulação, identificação paramétrica e aplicação com emprego do método dos elementos finitos,” M.S. thesis, Univ. São Paulo, São Carlos, 1993.

[72] L. G. L. Costa, W. C. Santiago, and A. T. Beck, "Probabilistic models for live loads in buildings: critical review, comparison to Brazilian design standards and calibration of partial safety factors," *Rev. IBRACON Estrut. Mater.*, vol. 16, no. 2, pp. 1–21, 2023, http://doi.org/10.1590/s1983-41952023000200004.

[73] M. Otieno, H. Beushausen, and M. Alexander, "Prediction of corrosion rate in reinforced concrete structures: a critical review and preliminary results," *Mater. Corros.*, vol. 63, no. 9, pp. 777–790, 2012, http://doi.org/10.1002/maco.201106282.

Author contributions: Chiara P. Teodoro: conceptualization, data curation, formal analysis, methodology, writing. Rogério Carrazedo: conceptualization, supervision, writing.

Editors: José Marcio Calixto, Daniel Cardoso.